UNIVERSITY OF AMSTERDAM

UvA-DARE (Digital Academic Repository)

Control analysis of glycolytic oscillations.

Bier, M.; Teusink, B.; Kholodenko, B.N.; Westerhoff, H.V.

Control analysis of glycolytic oscillations

Martin Bier [a], Bas Teusink [b], Boris N. Kholodenko [c], Hans V. Westerhoff [d,e,*]

[a] *University of Chicago, Dept. of Surgery MC 6035, Sect. of Plastic and Reconstructive Surgery, Chicago IL 60637, USA*
[b] *E.C. Slater Institute, BioCentrum, University of Amsterdam, Amsterdam, The Netherlands*
[c] *A.N. Belozersky Institute of Physico-Chemical Biology, Moscow State University, Russian Federation*
[d] *The Netherlands Cancer Institute / AvL, H5, Amsterdam, The Netherlands*
[e] *Vrije Universiteit, Faculty of Biology, Dept. of MicroPhysiology, de Boelelaan 1087, NL-1081 HV Amsterdam, The Netherlands*

Abstract

The principles involved in the control of the frequency of sustained metabolic oscillations are developed in the context of glycolytic oscillations in *Saccharomyces cerevisiae*. To this purpose, an existing mathematical model that describes the experimentally obtained oscillations was simplified to a core model. Frequency, relative phase, average concentrations and amplitudes of the oscillations were well approximated by writing the two remaining metabolic variables of the core model (representing [ATP] and [hexose]) as harmonic functions of time and by requiring them to fulfill the differential equations.

The extent to which an enzyme (-conglomerate) controls the frequency in a sustained oscillation is defined as the log–log derivative of that frequency with respect to enzyme activity. In both the full model and the core model this control of frequency and the control over the average concentrations proved to be distributed over the enzymes. We identified a summation theorem, stating that the sum of such control coefficients over all processes equals unity for frequency and zero for the average concentrations.

Keywords: Control analysis; Glycolytic oscillations

1. Introduction

Periodic phenomena are known to be critically involved in a number of cases of multicellular organization [1]. Within single cells both the occurrence and the significance of metabolic oscillations is much less well documented. For one of the best studied systems of eukaryotic cell metabolism, i.e. that of the yeast *Saccharomyces cerevisiae*, oscillations in NAD(P)H fluorescence and concentrations of glycolytic intermediates have only been reported under

a limited number of conditions, such as anaerobiosis or cyanide poisoning subsequent to glucose feeding after starvation [2,3]. This has led to the conjecture that (i) the regulatory features necessary for appropriate control of metabolic pathways such as glycolysis lead to a potential for the occurrence of dynamic behavior that extends beyond the steady state and that (ii) the cell has additional regulatory aspects that prevent the undesired metabolic oscillations from occurring [4]. In this view the physiological state is a steady state and only under conditions where the homeostatic regulatory mechanisms are compromised, the "pathological" oscillating conditions arise. Indeed, earlier and subsequent experimental

* Corresponding author (at Vrije Universiteit, Faculty of Biology). Fax: +31 20 4447229.

studies have suggested that the glycolytic oscillations in yeast are sensitive to changes in the activities of some enzymes, including those involved in free-energy metabolism [5,6]. And, the tendency of the cells to oscillate depends strongly on their "make-up", as the latter changes in the transition between using glucose and using ethanol as the substrate [7,8]; the cells oscillate longest when harvested at that transition point, where perhaps metabolism is between two opposing control regimens and hence, less than optimally, buffered against oscillations. An additional factor of importance is the communication between individual cells [7,9–11].

Various conceptual frameworks have been developed to deal with the control of concentrations and fluxes at steady state. Of these, metabolic control theory (MCT) [12–15] offers a quantitative definition of the extent to which the fundamental biochemical entities in a metabolic pathway, i.e. the enzymes, control fluxes and concentrations. Theorems interrelating these control coefficients and relating them to enzyme properties make it possible to understand steady state control in terms of the individual properties of the enzymes in the system and their networking [14–16]. This MCT focuses on steady state because it is precisely the homeostatic properties of this state that are responsible for some of the important control properties, which can be expressed into theorems [14,17,18]. For transient phenomena some of the corresponding theorems are lacking (but see Refs. [14,18,19]).

Sustained (limit-cycle) oscillations are in fact stationary states and do exhibit homeostatic properties [20]. Consequently, it may be possible to develop something like the MCT for steady states also for limit-cycle oscillations. Following up on earlier work defining the control coefficients for the frequency of the oscillations [13,21–24], we here develop a simple but realistic computer model for glycolytic oscillations in yeast [25]. Baconnier, Pachot and Demongeot have performed numerical studies and a control analysis on a model of glycolytic oscillations [25]. In their model the oscillations originate in the AMP effect on the phosphofructokinase activity. They showed that the control of the enzyme activities on amplitudes and period is often complicated, capricious and unpredictable. In contrast to most metabolic control analysis, these authors focused on the control

by inhibitors, rather than on control by enzymes [12,14] or catalytic activities [13,26,27]. Here we shall focus on the control by the enzymes, as these are the normal biological agents which the cell can adjust by adjusting gene expression [22]. In addition, our model is centered around the positive feedback of ATP on its own rate of production and is mathematically a lot simpler. Consequently its behavior can, to a large extent, be followed in terms of simple analytic formulae. Using this simple model we shall illustrate and test definitions and theorems concerning the amplitude and frequency of the oscillations. In addition the control properties of limit cycles arising close to the Hopf bifurcation, are derived analytically. As in the control of steady state fluxes, control tends to be distributed among many factors. Summed over all the catalytic steps, control on frequency and average concentrations adds up to 100 and 0% respectively.

2. Methods

2.1. Computer models

To describe glycolytic oscillations in yeast we employed both an extended and a core model. The former was based on models [10,28] that were previously shown to describe experimentally observed oscillations in NADH fluorescence:

$$v_1(T,G) = k_1 TG$$
$$v_3(T,I,H) = k_3(C_{AD} - T)I(P_{tot} - I - T)(C_N^{tot} - H)$$
$$v_5(I,H) = k_5 IH/(K_H + H)$$
$$v_7(P,H) = k_7 PH/(H + K_{HP})$$
$$v_8(E,H) = k_8 E(C_N^{tot} - H)$$
$$v_9(T) = k_9 T$$
$$v_{11}(A,T) = k_{11} AT$$
$$v_p(T) = k_p T/(K_M + T)$$
$$v_N(H) = k_N H/(H + K_{HO})$$

The rates refer to the processes indicated in Fig. 1. Concentrations are those for ATP (T), NADH (H), intracellular glucose or any other relevant hexose (G), triose phosphates (I), ethanol (E), pyruvate (P) and acetate (A), respectively. Sum concentrations C_{AD} for adenine nucleotides, C_N^{tot} for nicotinamide adenine dinucleotides and P^{tot} for total phosphate were assumed to be constant. The time deriva-
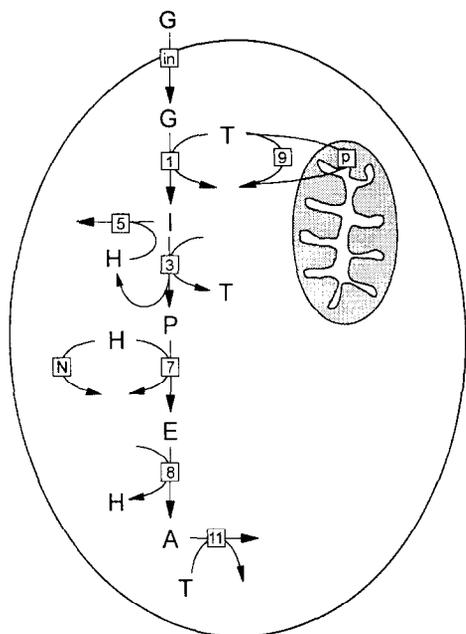
Fig. 1. The full model of the glycolysis which leads to the system of six coupled ordinary differential equations described in Section 2.1.

tives of the concentrations are related to the process rates (v) by:

$G'(t) = V_{in} - v_1$

$T'(t) = -2v_1 + 2v_3 - v_9 - v_p - v_{11}$

$I'(t) = 2v_1 - v_3 - v_5$

$H'(t) = v_3 - v_7 + 2v_8 - v_N - v_5$

$P'(t) = v_3 - v_7$

$E'(t) = 0$

$A'(t) = v_8 - v_{11}$

These equations were integrated numerically using MLAB (Civilized Software, Bethesda, MD), or STELLA (timestep 0.1, Runge Kutta 4th order).

The core model corresponds to an agglomeration of processes of the extended model into three modules: (i) import of glucose at rate V_{in}, (ii) glycolysis coupled to the production of two molecules of ATP at rate $2k_2GT$ and (iii) ATP hydrolysis with both a saturable $[-k_pT/(K_m + T)]$ and a nonsaturable $(-k_9T)$ component:

$$\frac{dG}{dt} = V_{in} - k_2GT$$

$$\frac{dT}{dt} = 2k_2GT - k_p\frac{T}{K_m + T} - k_9T \qquad (1)$$

2.2. Experimental

Yeast glycolytic oscillations were induced as described [8]. Essentially, *S. cerevisiae* was grown on glucose until the latter had been depleted. The cells were then harvested and washed in phosphate buffer at room temperature. In that same buffer they were then starved for two hours at 30°C without forced aeration. Subsequently the cells were incubated at a concentration corresponding to approximately 5 mg protein ml^{-1} in phosphate buffer at 20°C, provided with 20 mM glucose and 4 min later with 4 mM KCN. Oscillations were monitored through NAD(P)H fluorescence (see Refs. [8,11]).

3. Results

3.1. Development of a core model describing the experimentally observed sustained glycolytic oscillations

Fig. 2 shows the time dependence of NADH fluorescence when *S. cerevisiae* was harvested around the transition between glycolysis and ethanol oxidation, starved for 2 h, and then given glucose and cyanide. Upon cyanide addition, oscillatory be-
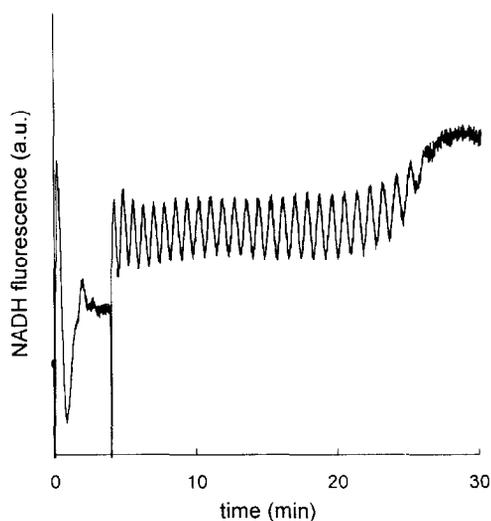

Fig. 2. Experimental oscillations on intact yeast cells monitored through the NAD(P)H fluorescence. At $t = 0$, 20 mM glucose was added, followed by 4 mM KCN at $t = 4$ min.

havior is observed; the first few cycles show transient oscillations that were irreproducible between different batches of cells, and that relax to a sustained oscillation with constant amplitude and frequency [8,9]. In Fig. 2, the transient behavior is seen as a decrease in frequency until the constant, limit-cycle frequency is observed. In some batches of cells, also the amplitude of the oscillations changed in this transient phase. Meanwhile, pyruvate and ethanol concentrations increased virtually monotonically. During the case of sustained oscillations in NADH, also the concentrations of the adenine nucleotides, and the hexose phosphates oscillated [24].

Fig. 3 shows the eventual limit cycle in a simulation of the full model. The initial behavior of NADH fluorescence depended rather strongly on the initial perturbation (not shown), whereas the frequency and amplitude of the sustained oscillation that was ultimately obtained, did not. This corresponds with the experimental results. The relative independence of the ultimate, sustained oscillations on the initial conditions, is the reason why we shall focus on sustained oscillations and their control (see Ref. [8]).

The model used to obtain Fig. 3 is rather complicated; it contains six metabolically independent variables. For a model to illustrate the principles of the control of glycolytic oscillations, this complexity is undesirable. We shall now examine if the model may

be reduced in complexity without much affecting the oscillations it simulates.

Fig. 3 shows that in the final limit cycle oscillation, both the average concentration and the time dependence of the concentration of the triose-phosphates was small compared to those of most other metabolites. More specifically, $\frac{dI}{dt} + v_5$ was much smaller than both v_3 and v_1. This suggested to simplify the model by neglecting the flux of carbon towards glycerol (v_5), allowing us to take $v_3 = 2v_1$ and thus to eliminate v_3 from the expression for the time dependence of T.

Secondly, the calculations with the complete model showed that v_{11} was always at least seven times smaller than v_1, v_g and v_p, such that within the limit of experimental accuracy, v_{11} may be neglected in the equation for the time dependence of T.

As a consequence of these two simplifications, the differential equations for G and T decouple from the other differential equations. This leads to Eq. (1).

Fig. 4 compares the simulation of the time dependence of G and T obtained with the core model, to the simulation obtained with the extended model. The full model oscillated around (5.0, 1.0) and at a radial velocity of $\omega = 0.140$. The reduced model oscillated around (4.7, 0.99) with an $\omega = 0.141$: the frequency and center of the oscillations generated by
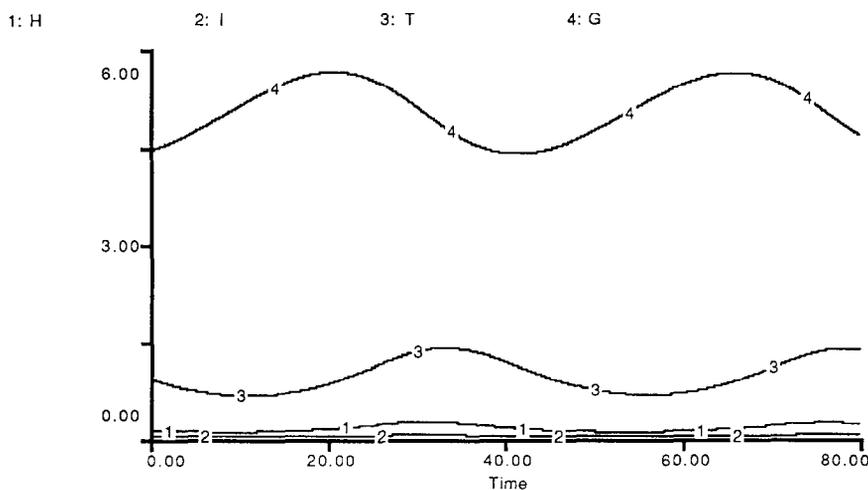
Fig. 3. A simulation of the full model of Fig. 1 with $V_m = 0.24$, $k_1 = 0.05$, $k_3 = 0.05$, $k_5 = 0.4$, $k_7 = 0.1$, $k_8 = 0.001$, $k_9 = 0.3$, $k_{11} = 0.02$, $K_H = 0.02$, $K_{HP} = 0.2$, $K_m = 2$, $k_{HO} = 0.2$, $k_p = 0.5$, $k_N = 0.08$, $C_{AD} = 8$, $P_{tot} = 10$, $C_N^{tot} = 8$, $E = 2$. Shown are the oscillating concentrations of NADH (1), triose phosphates (2), ATP (3) and hexose (4) after the system had relaxed to its limit cycle.
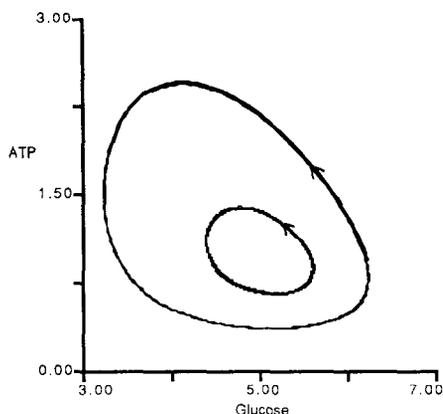
Fig. 4. The hexoses versus ATP phase-plane behavior for the full model (small cycle) and the core model (large cycle).

the extended and the core model were similar, whereas the amplitudes of oscillation differed considerably.

An important consideration is that the core model produced a limit cycle (see below). Limit cycles (e.g. as opposed to oscillations in the Lotka–Volterra model) are structurally stable. Consequently, the reactions neglected in the core model may slightly affect the frequency and shape of the limit cycle, but they do not affect the limit cycle behavior as such.

According to Nicolis and Prigogine [20] a "necessary ingredient" to an oscillating chemical reaction with two variable concentrations is a nonlinearity of third or higher order. In our case one quadratic nonlinearity arises from the involvement of ATP in a positive feedback loop (see Refs. [28,29]). The first step in the breakdown of glucose involves the dephosphorylation of two molecules of ATP. Once this step has been taken, the further breakdown of glucose generates four ATPs. A higher order nonlinearity comes about through the Michaelis–Menten term for the saturable ATPase.

3.2. Analytical description of the limit cycle behavior of the core model

In this section we will derive expressions that relate the frequency, amplitude and phase of the oscillations in G and T, to the system parameters. In principle any periodic solution can be quantitatively captured to any desired degree of accuracy by substi-

tuting a Fourier series and going to sufficiently high order. In Figs. 2–4 the oscillations appear smooth and harmonic, which induces us to truncate the series after the first term, i.e. we substitute a harmonic oscillation. After some relatively simple algebra this will lead us to formulae that express in terms of parameter values the frequency, phase difference, averages and amplitudes of the G and T oscillations. Subsequently we can check the accuracy of the obtained expressions against the result of numerical simulations of the core model of Eq. (1). Hence:

$$G = \gamma_0 + \gamma_1 e^{i\omega t} + \gamma_{-1} e^{-i\omega t}$$

$$T = \theta_0 + \theta_1 e^{i\omega t} + \theta_{-1} e^{-i\omega t} \tag{2}$$

with $\theta_1 = \theta_{-1}$, γ_0 and $\theta_0 \in R^+$ (i.e. we take for $t = 0$ the moment at which the T oscillation is at its maximum) and $\gamma_1 = \gamma_{-1}^*$ (an asterisk denotes complex conjugation). One has for the $k_p T / (K_m + T)$ nonlinearity:

$$k_p \left(\frac{T}{K_m + T} \right) = \frac{k_p}{K_m} T \left(\frac{1}{1 + (T/K_m)} \right)$$

$$= \frac{k_p}{K_m} \left(\theta_0 + \theta_1 e^{i\omega t} + \theta_1 e^{-i\omega t} \right)$$

$$\times \left(\frac{1}{1 + \frac{\theta_0}{K_m} + \frac{\theta_1}{K_m} e^{i\omega t} + \frac{\theta_1}{K_m} e^{-i\omega t}} \right)$$

We shall now assume that the $(1 + \theta_0/K_m)$ term dominates the denominator. Using $1/(a + \epsilon) \approx (a - \epsilon)/a^2$ we obtain:

$$k_p \frac{T}{K_m + T} \approx \frac{k_p}{K_m} \frac{1}{[1 + (\theta_0/K_m)]^2}$$

$$\times \left\{ \left[\theta_0 \left(1 + \frac{\theta_0}{K_m} \right) - \frac{2}{K_m} \theta_1^2 \right] \right.$$

$$\left. + \frac{\theta_1}{K_m} e^{i\omega t} + \frac{\theta_1}{K_m} e^{-i\omega t} \right\} \tag{3}$$

In the calculations corresponding to Figs. 3 and 4, $\theta_1 \approx 0.2$ and $\theta_0 \approx 1$, which leads to $a = 1.5$ and $\epsilon = 0.2$ (at $t = 0$ when ϵ is maximal). For such values the approximation has an inaccuracy of less than 2%.

From the system of Eq. (1) it follows that:

$$2\frac{dG}{dt} + \frac{dT}{dt} = 2V_{in} - k_p \frac{T}{K_m + T} - k_9 T$$

Substituting the expression for G and T (i.e., Eq. (2)) into this equation as well as into the first part of Eq. (1), using Eq. (3) and equating at zeroth order one finds:

$$2V_{in} - \frac{k_p}{(K_m + \theta_0)^2} \left[\theta_0(\theta_0 + K_m) - 2\theta_1^2 \right] - k_9 \theta_0$$

$$= 0 \qquad (4a)$$

$$k_1(\gamma_1 + \dot{\gamma}_1)\theta_1 = V_{in} - k_1 \gamma_0 \theta_0 \qquad (4b)$$

Equating at first order leads to:

$$\begin{pmatrix} 2i\omega & \frac{k_p K_m}{(\theta_0 + K_m)^2} + k_9 + i\omega \\ k_1\theta_0 + i\omega & k_1\gamma_0 \end{pmatrix} \begin{pmatrix} \gamma_1 \\ \theta_1 \end{pmatrix}$$

$$= \begin{pmatrix} 0 \\ 0 \end{pmatrix} \qquad (5)$$

Nonzero solutions for γ_1 and θ_1 are obtained only if the determinant of the matrix equals zero. This leads to two equations, one for the real part and one for the imaginary part of the requirement that the determinant is zero:

$$\omega^2 = \frac{k_1 k_p K_m \theta_0}{(K_m + \theta_0)^2} + k_1 k_9 \theta_0 \qquad (6a)$$

$$k_1(2\gamma_0 - \theta_0) = \frac{k_p K_m}{(\theta_0 + K_m)^2} + k_9 \qquad (6b)$$

The former equation gives an expression for ω (2π times the frequency) in terms of system parameters and the average concentration of T.

For our choice of parameters the fixed point (G_0, T_0; the point where the time derivatives are zero) appears to be very close to the center of the harmonic oscillation (γ_0, θ_0). For the parameter values used to obtain Figs. 3 and 4:

$$(G_0, T_0) = (4.65, 1.03)$$

The average magnitudes of G and T turned out to be 5.0 and 1.0 respectively. Substituting the values (G_0, T_0) for (γ_0, θ_0) seems to be reasonable as a

zeroth order approximation. This leads to an estimate (using Eq. (6a)) for ω of

$$\omega = 0.145 \, s^{-1}$$

which differs by less than 5% from the observed ω of 0.14 s^{-1} of the full model (Fig. 3; see Ref. [8]). The variables A, H, I and P oscillate with the same frequency and their behaviour appears to be "driven" by the limit cycle oscillation of T and G.

From the first row of Eq. (5) we have:

$$\gamma_1 = \left\{ -\frac{1}{2} + \left(\frac{k_p K_m}{2\omega(K_m + \theta_0)^2} + \frac{k_9}{2\omega} \right)i \right\} \theta_1 \qquad (7)$$

The absolute value of the number in braces is the ratio of the amplitude of the oscillations in G and T. For the parameter values of Fig. 3, the number within the braces is $(-0.5 + (1.45)i)$ which has an absolute value of 1.5. The values observed in the simulation are $|\theta_1| = 0.2$ and $\gamma_1 = 0.35$ which means a 10% inaccuracy for Eq. (5).

The phase difference between the G- and the T oscillation is:

$$\Delta\varphi = \pi - \arctan\left\{ \frac{k_p K_m}{\omega(K_m + \theta_0)^2} + \frac{k_9}{\omega} \right\} \qquad (8)$$

This formula predicts the G oscillation to be 1.9 rad (108°) ahead of the T oscillation. This corresponds to the results of Figs. 3 and 4.

From Eq. (7) it follows that $\gamma_1 + \gamma_1^* = -\theta_1$. Combining this with Eq. (4b), $k_1\theta_1^2 = k_1 \gamma_0 \theta_0 - V_{in}$. This formula relates the averages of T and G to the amplitude of T. It is readily seen that if (γ_0, θ_0) is the location of the fixed point, θ_1^2 comes out to be zero.

Substituting $k_1\theta_1^2 = k_1 \gamma_0 \theta_0 - V_{in}$ in Eq. (4a) one obtains:

$$2V_{in} - \frac{k_p}{(K_m + \theta_0)^2} \left(\theta_0(\theta_0 + K_m) \right.$$

$$\left. + \frac{2V_{in}}{k_1} - 2\gamma_0 \theta_0 \right) - k_9 \theta_0 = 0 \qquad (9)$$

If one combines this equation with Eq. (6b), one obtains a nonlinear algebraic system which can be solved (for instance with an iterative method) for the average concentrations γ_0 and θ_0, given only parameter values. With $k_1\theta_1^2 = k_1 \gamma_0 \theta_0 - V_{in}$ an esti-

mate of the amplitude of the limit cycle in T can be derived.

An ordinary linear eigenvalue analysis at the fixed point would have given Eq. (5), and Eqs. (6a), (6b)–(8) which are consequences of Eq. (5). Our approach gives the equations under Eqs. (4a) and (4b) and the resulting Eq. (9) as an extra. Eqs. (4a), (4b) and (5) together lead to estimates for (γ_0, θ_0), i.e. averages of the G and T oscillations, and the amplitudes γ_1 and θ_1. In the standard linear analysis one substitutes the values of the fixed point (G_0, T_0) into Eq. (6a) to obtain an estimate for the frequency. By substituting θ_0 into Eq. (6a) instead of the fixed point T_0, we can obtain a first correction. Furthermore, our analysis points the way to further expansion and concurrent higher accuracies. Any desired accuracy can be achieved by truncating the Fourier series Eq. (2) at a sufficiently high order. In this way we can also describe waveforms that are different from the harmonic shape that we have restricted ourselves to here. The higher accuracy, however, also means that increasingly complicated algebraic

systems have to be solved to obtain the Fourier components. The method of substitution of Fourier series can also be applied when the dynamical system consists of more than two equations, but the algebra will be correspondingly more laborious.

The other variables A, I, H and P follow the oscillations of the G,T system. Their oscillations can therefore be described by inserting the above derived approximations for $T(t)$ and $G(t)$ into the remaining equations, substituting harmonic functions of time (as in Eq. (2)) for A, I, H and P and equating at orders 0 and 1 in $e^{i\omega t}$.

We conclude that for most aspects, the harmonic oscillation represented by Eq. (2), is a fair representation of the oscillations of the core model.

3.3. Control analysis

In line with metabolic control analysis of steady state fluxes and concentrations, one may define the extent to which an enzyme (or process described in

Table 1

Control coefficient of some of the characteristics of the limit cycle of Eq. (1) with respect to the five parameters V_{in}, k_2, k_p, K_m, and k_9, at $V_{in} = 0.24$, $k_2 = 0.05$, $k_m = 2$, $k_9 = .3$, $k_p = 0.5$

Oscillation leaving fixed point of Eq. (1)	Limit cycle	
	Harmonic approximation according to Eqs. (2)–(4a), (4b)–(6a), (6b)–(9)	Simulation of Eq. (1)
$(G_0,T_0) = (4.65, 1.03)$	$(\gamma_0, \theta_0) = (4.58, 1.21)$	$(\gamma_0, \theta_0) = (4.73, 1.07)$
$\omega = 0.145$	$\Omega = 0.155$	$\Omega = 0.141$
$C_{V_{in}}^{\omega} = 0.46565$	$C_{V_{in}}^{\Omega} = 0.498756$	$C_{V_{in}}^{\Omega} = 0.615$
$C_{k_2}^{\omega} = 1/2$	$C_{k_2}^{\Omega} = 0.498756$	$C_{k_2}^{\Omega} = 0.565$
$C_{k_p}^{\omega} = -0.0321337$	$C_{k_p}^{\Omega} = 0.000108$	$C_{k_p}^{\Omega} = -0.208$
$C_{K_m}^{\omega} = 0.066484$	$C_{K_m}^{\Omega} = 0.000000$	$C_{K_m}^{\Omega} = 0.239$
$C_{k_9}^{\omega} = 0.066484$	$C_{k_9}^{\Omega} = 0.000008$	$C_{k_9}^{\Omega} = 0.0018$
$C_{V_{in}}^{G_0} = -0.137346$	$C_{V_{in}}^{\gamma_0} = -0.032824$	$C_{V_{in}}^{\gamma_0} = -0.153$
$C_{k_2}^{G_0} = -1.$	$C_{k_2}^{\gamma_0} = -0.859329$	$C_{k_2}^{\gamma_0} = -0.949$
$C_{k_p}^{G_0} = 0.403383$	$C_{k_p}^{\gamma_0} = 0.221168$	$C_{k_p}^{\gamma_0} = 0.393$
$C_{K_m}^{G_0} = -0.266038$	$C_{K_m}^{\gamma_0} = -0.0544749$	$C_{K_m}^{\gamma_0} = -0.285$
$C_{k_9}^{G_0} = 0.733962$	$C_{k_9}^{\gamma_0} = 0.681937$	$C_{k_9}^{\gamma_0} = 0.706$
$C_{V_{in}}^{T_0} = 1.13735$	$C_{V_{in}}^{\theta_0} = 1.22735$	$C_{V_{in}}^{\theta_0} = 0.928$
$C_{k_2}^{T_0} = 0$	$C_{k_2}^{\theta_0} = 0.000000$	$C_{k_2}^{\theta_0} = -0.196$
$C_{k_p}^{T_0} = -0.403383$	$C_{k_p}^{\theta_0} = -0.299248$	$C_{k_p}^{\theta_0} = -0.09$
$C_{K_m}^{T_0} = 0.266038$	$C_{K_m}^{\theta_0} = 0.0740945$	$C_{K_m}^{\theta_0} = -0.104$
$C_{k_9}^{T_0} = -0.733962$	$C_{k_9}^{\theta_0} = -0.916717$	$C_{k_9}^{\theta_0} = -0.668$
$\Sigma C_{e_i}^{\omega} = 1.00000$	$\Sigma C_{e_i}^{\Omega} = 0.997628$	$\Sigma C_{e_i}^{\Omega} = 0.973$
$\Sigma C_{e_i}^{G_0} = 0.00000$	$\Sigma C_{e_i}^{\gamma_0} = 0.0109523$	$\Sigma_{e_i}^{\gamma_0} = 0.003$
$\Sigma C_{e_i}^{T_0} = 0.00000$	$\Sigma C_{e_i}^{\theta_0} = 0.0113827$	$\Sigma C_{e_i}^{\theta_0} = -0.026$

Refs. [26,27,30]) controls the frequency of the limit cycle oscillation by [21,22,25,31–33]:

$$C_{e_i}^{\omega} = \frac{\mathrm{d}\ln(\omega)}{\mathrm{d}\ln(e_i)}$$

In our core model the parameters V_{in}, k_1, k_p and k_9 are proportional to the concentration of the corresponding enzymes (or conglomerates thereof). Similarly the control by other parameters such as K_m may be defined. In general the control (response) coefficient with respect to any parameter p is [34]:

$$C_p^{\omega} = \frac{\mathrm{d}\ln(\omega)}{\mathrm{d}\ln(p)}$$

The control, (i) of the amplitudes of the limit cycle of T and G, (ii) of the average concentrations of T and G, and (iii) of the phase difference between T and G, by any parameter p are defined analogously. These control coefficients can be expressed in the values of all parameters of the system by differentiating the equations derived in the preceding section with respect to the corresponding parameters and evaluating the resulting expressions.

Table 1 presents the various control coefficients evaluated numerically for the core model (third column), calculated analytically for the harmonic approximation to the core model (middle column) and calculated for the fixed point of the core model (first column).

At the Hopf bifurcation the fixed point and the center of oscillation coincide. When the parameters V_{in}, k_1, k_p, K_m and k_9 are changed to move away from the Hopf bifurcation the fixed point and the center of oscillation move apart. C_p^{G0} and C_p^{T0} tell us how readily the fixed point is changing location as parameter p is varied. Thus $(C_p^{G0} - C_p^{\gamma 0})$ and $(C_p^{T0} - C_p^{\theta 0})$ are a measure for how readily the fixed point and the center of oscillation are moving away from each other. For our limit cycle, (G_0, T_0) approximates the location of (γ_0, θ_0) rather well (see above), whereas the coefficients for the control on (G_0, T_0) differ very much from those on (γ_0, θ_0). The same argument holds when one compares the radial velocity ω of the outgoing spiral around the fixed point according to Eq. (6a) with the actual radial velocity Ω of the limit cycle.

When we take the parameter values that we use in the figures ($V_{\mathrm{in}} = 0.24$, $k_1 = 0.05$, $K_\mathrm{m} = 2$, $k_9 = 0.3$, $k_\mathrm{p} = 0.5$) and solve Eq. (6b) and Eq. (9) for θ_0 and γ_0, we get the values in the first line of Table 1. With $\theta_1^2 = \gamma_0 \theta_0 - V_{\mathrm{in}}/k_1$ this leads to $\theta_1 = 0.86$. In Fig. 4 we see that the actual value is 0.5. We have not listed the control coefficients on the amplitude in Table 1. The values for C_p^{G0}, C_p^{T0}, C_p^{ω} and $C_p^{\gamma 0}$, $C_p^{\theta 0}$, C_p^{Ω} where p stands for V_{in}, k_1, k_p, K_m and k_g respectively are listed in Table 1.

The control coefficients for G_0, T_0 and ω were evaluated analytically with MATHEMATICA and those for γ_0, θ_0 and Ω were obtained through solving Eqs. (6b) and (9) with an iterative scheme (middle column) and numerically through simulation using MLAB (third column). For both the middle and third columns, the value of a parameter p was changed by 1% and the corresponding change in γ_0, θ_0 and Ω was calculated.

Influx, feedback and efflux steps are all equally essential in a limit cycle. Table 1 shows how the controls are evenly distributed. V_{in}, k_1, k_p and k_g are all inversely proportional to time. So the summation of the controls on the radial velocity with respect to these parameters should yield one and summation of the controls on G_0, T_0 and γ_0, θ_0 with respect to these parameters should be zero, i.e.:

$$\Sigma C_{e_i}^{\omega} = 1, \ \Sigma C_{e_i}^{\Omega} = 1, \ \Sigma C_{e_i}^{G_0} = 0, \ \Sigma C_{e_i}^{T_0} = 0 \qquad (10)$$

$$\Sigma C_{e_i}^{\gamma_0} = 0, \ \Sigma C_{e_i}^{\theta_0} = 0, \ e_i = V_{\mathrm{in}}, k_1, k_\mathrm{p}, k_9$$

These equations hold because the simultaneous change of V_{in}, k_1, k_p and k_9 by the same factor amounts to a scaling of the time. This should affect the radial velocity but not the positions (G_0, T_0) and (γ_0, θ_0) [14,21,35]. These theorems are not exactly reflected by the calculations of the middle and third columns of Table 1 because we approximated C_{ei}^x by changing e_i by 1% and calculating the new value of Eq. (10).

The discrepancy between the second and third columns occurs because the calculations leading to Eqs. (6a), (6b) and (9) did not take second- and higher-order Fourier terms into account. Indeed, Fig. 4 shows that the limit cycle does not look perfectly ellipsoidal. Eqs. (6b) and (10) are perfect approximations when the limit cycle is infinitesimally small very close to the Hopf bifurcation. But for physically

relevant oscillations as in Fig. 2, the higher order Fourier components have a nonnegligeable effect on the control coefficients.

4. Discussion

In this paper we have developed parts of a control analysis of metabolic oscillations. We defined the coefficients quantifying the control exercised by enzymes and kinetic parameters on the properties that characterize limit cycles. We also identified summation theorems for these properties. Our approach was analytical, using a numerical model by way of illustration.

The definitions of the control coefficients are analogous to the coefficients defined to describe the control of a steady-state flux [34]. Accordingly the summation theorems take similar forms. With respect to the control of frequency [13,21,22,25] and of amplitude [13,22,25] the present treatment corresponds to and extends earlier work. The definitions should apply to any limit cycle of any size and form. The theorems are also valid for the general case. This is so irrespective of the fact that we here applied them to the particular case of harmonic glycolytic oscillations, close to a Hopf bifurcation. Indeed, to ensure the practicability of the approach we developed it with frequent reference to the experimental system where we observe sustained metabolic oscillations, i.e. yeast glycolysis [8,36]. We employed a comprehensive model for those oscillations and showed that it describes essential aspects of the experimental oscillations. We then simplified the model to a core model that still simulates the experimental results at an only slightly reduced accuracy. For the core model we could derive approximations for frequency and phase difference. We then demonstrated how the control coefficients can be calculated from the parameter values once one has a complete kinetic model.

The limit cycle of the core model contains two nonlinear characteristics: the positive feedback of ATP on its own production rate and the Michaelis–Menten type of saturability of the ATP breakdown reaction by the concentration of ATP. Replacing the latter by a power law approximation [37] $(T/(K_m + T)) \approx \sqrt{(T)}/(2\sqrt{(K_m)})$ did not produce a limit cycle

(not shown). Earlier it was shown for a similar model that the positive feedback of ATP on its own production rate was essential for the limit cycle behaviour of that model [28].

This core model differs from other core models in the literature: the one developed by Sel'kov and coworkers (see Ref. [38]) has a third power concentration dependence ($v = kGT^2$) but no saturable kinetics. An autonomous system of two coupled ordinary differential equations with just quadratic nonlinearities cannot produce limit cycles. In our case the presence of the ATP concentration in the denominator (as $T + K_m$) is equivalent to having higher order dependencies on ATP concentration in the numerator, as is obvious from a Taylor expansion [see Ref. [28]]. The ATP hydrolysis term that is linear in ATP concentration ($k_g T$) is not necessary for limit cycle behavior but we kept it to obtain a good approximation to the full model.

The model for glycolytic oscillations developed by Goldbeter and others (see Ref.[39]) focuses on phosphofructokinase alone as the generator of the oscillation through the effect of AMP concentration on the enzyme and the corresponding nonlinearities. Sel'kov [40] focused on the lower part of glycolysis as the oscillophore. The model studied by Baconnier et al., [25] focuses on phosphofructokinase and pyruvate kinase. It did exhibit distributed control (by inhibitors) differently for amplitude and period. At the Hopf bifurcation the behaviour was discontinuous however, which together with its analytical complexity made it unsuitable for the analytical analysis we performed in the present manuscript.

Without detracting from the value of these two models in delineating crucial aspects of the oscillations, we now may be entering an era where it becomes possible, in line with metabolic control analysis, to see also experimentally if control by enzymes is distributed over many steps or confined to a single step (see also [41–43]). Our calculated values of the control coefficients (compare Ref. [25]) suggest that in the case of oscillations, control may be distributed (see Refs. [25,44]) and that it may be fruitful to ask how and why the control (e.g. of the frequency) is distributed over all processes and regulatory interactions in the system.

Another interesting feature that appears from the calculated control coefficients shown in the table is

that if one aspect of an oscillation is controlled by a certain (combination of) enzyme(s), this does not imply that all other aspects of the oscillations are also controlled by that enzyme. For instance whereas k_9 strongly controlled the average G and T it hardly controlled the frequency [44].

Acknowledgements

References

[1] A. Goldbeter, Cell-to-Cell Signalling, Academic Press, New York, 1989.
[2] A. Ghosh and B. Chance, Biochem. Biophys. Res. Commun., 204 (1964) 118–123.
[3] B. Hess and A. Boiteux, Annu. Rev. Biochem., 40 (1971) 237–258.
[4] H.V. Westerhoff, M.A. Aon, K. van Dam, S. Cortassa, D. Kahn and M. van Workum, Biochim. Biophys. Acta, 1018 (1990) 142–146.
[5] A.K. Ghosh, B. Chance and E.K. Pye, Arch. Biochem. Biophys., 145 (1971) 319–331.
[6] M.A. Aon, S. Cortassa, H.V. Westerhoff, J.A. Berden, E. van Spronsen and K. van Dam, J. Cell Sci., 99 (1991) 325–334.
[7] E.K. Pye, Can. J. Bot., 47 (1969) 271–285.
[8] P. Richard, B. Teusink, H.V. Westerhoff and K. van Dam, FEBS Lett., 318 (1993) 80–82.
[9] J. Aldridge and E.K. Pye, Nature, 259 (1976) 670–671.
[10] M.A. Aon, S. Cortassa, H.V. Westerhoff and K. van Dam, J. Gen. Microbiol., 138 (1992) 2219–2227.
[11] P. Richard, J.A. Diderich, B.M. Bakker, B. Teusink, K. van Dam and H.V. Westerhoff, FEBS Lett., 341 (1994) 223–226.
[12] H. Kacser and J.A. Burns, Symp. Soc. Exp. Biol., 27 (1973) 65–104.
[13] R. Heinrich, S.M. Rapoport and T.A. Rapoport, Prog. Biophys. Mol. Biol., 32 (1977) 1–83.
[14] H.V. Westerhoff and K. van Dam, Thermodynamics and Control of Biological Free Energy Transduction, Elsevier, Amsterdam, 1987.
[15] D.A. Fell, Biochem. J., 286 (1992) 313–330.
[16] H.V. Westerhoff, J.-H. Hofmeyr and B.N. Kholodenko, Biophys. Chem., 50 (1994) 273–283.
[17] H.V. Westerhoff and Y. Chen, Eur. J. Biochem., 142 (1984) 425–430.
[18] D. Kahn and H.V. Westerhoff, Biotheoret. Acta, 41 (1993) 85–96.
[19] R. Heinrich and C. Reder, J. theor. Biol., 151 (1991) 343–350.
[20] G. Nicolis and I. Prigogine, Self-organization in nonequilibrium systems, John Wiley, New York, 1977.
[21] L. Acerenza, in A. Cornish-Bowden and M.-L. Cardenas (Eds.), Control of Metabolic Processes, Plenum Press, New York, 1990, pp. 297–302.
[22] H.V. Westerhoff, J.G. Koster, M. van Workum and K.E. Rudd, in A. Cornish-Bowden and M.-L. Cardenas (Eds.), Control of Metabolic Processes, Plenum Press, New York, 1990, pp. 399–412.
[23] M. Markus and B. Hess, Nature, 347 (1990) 56.
[24] P. Richard, B. Teusink, M.B. Hemker, K. van Dam and H.V. Westerhoff, Yeast, 12 (1996) 731–740.
[25] P.F. Baconnier, P. Pachot and J. Demongeot, J. Biol. Syst., 1 (1993) 335–347.
[26] S. Schuster and R. Heinrich, Biosystems, 27 (1992) 1–15.
[27] B.N. Kholodenko, D. Molenaar, S. Schuster, R. Heinrich and H.V. Westerhoff, Biophys. Chem., 56 (1995) 215–226.
[28] S. Cortassa, M.A. Aon and H.V. Westerhoff, Biophys. J., 60 (1991) 794–803.
[29] S. Cortassa, M.A. Aon and D. Thomas, FEMS Microbiol. Lett., 66 (1990) 249–256.
[30] B.N. Kholodenko, Biochemistry (USSR), 58 (1993) 512–528.
[31] L. Acerenza, J. Theor. Biol., 165 (1993) 63–85.
[32] M. Markus and B. Hess, in A. Cornish-Bowden and M.-L. Cardenas (Eds.), Control of Metabolic Processes, Plenum Press, New York, 1990, pp. 303–316.
[33] H.V. Westerhoff, W.C. van Heeswijk, D. Kahn and D.B. Kell, Anth. van Leeuwenh., 60 (1991) 193–208.
[34] J.A. Burns, A. Cornish-Bowden, A.K. Groen, R. Heinrich, H. Kacser, J.W. Porteous, S.M. Rapoport, T.A. Rapoport, J.W. Stucki, J.M. Tager, R.J.A. Wanders and H.V. Westerhoff, Tr. Biochem. Sci., 10 (1985) 16.
[35] C. Giersch, Eur. J. Biochem., 174 (1988) 509–513.
[36] B. Hess and A. Boiteux, Ber. Bunsen Ges. Phys. Chem., 84 (1980) 346–351.
[37] M.A. Savageau, Biochemical Systems Analysis. A study of function and design in molecular biology, Addison-Wesley, Reading, MA, 1976.
[38] J. Reich and E.E. Sel'Kov, Energy Metabolism of the Cell, Academic Press, New York, 1981.
[39] A. Goldbeter and R. Lefever, Biophys. J., 12 (1972) 1302–1315.
[40] E.E. Sel'kov, FEBS Lett., 37 (1973) 342–345.
[41] O. Richter, A. Betz and C. Giersch, Biosystems, 7 (1975) 137–146.
[42] A. Groen, R. van der Meer, H.V. Westerhoff, R. Wanders, T. Akerboom and J. Tager, in H. Sies (Ed.), Metabolic compartmentation, Academic Press, London, 1982, pp. 9–37.
[43] H.V. Westerhoff, Tr. Biotechnol., 13 (1995) 242–244.
[44] B. Teusink, B.M. Bakker and H.V. Westerhoff, Biochim. Biophys. Acta, 1275 (1996) 204–212.